

# INFLUENCE OF THE PHOTOINJECTOR EXIT APERTURE ON THE WAKEFIELD DRIVEN BY AN INTENSE ELECTRON BEAM PULSE: A THEORETICAL APPROACH

J.-M. DOLIQUE, Université Joseph Fourier-Grenoble I, and CEA-Bruyères-le-Châtel. France

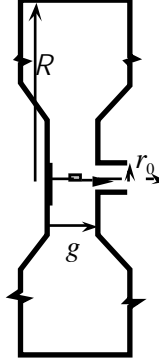
The wakefield generated in the cylindrical cavity of an RF photoinjector, by the strongly accelerated electron beam, has been analytically calculated [1] under the assumption that the perturbation of the field map by the exit hole is negligible as long as the ratio: exit hole radius/cavity radius is lower than approximately 1/3. Shown experimentally in the different context of a long accelerating structure formed by a sequence of bored pill-box cavities [2], this often quoted result must be checked for the wakefield map excited in a photoinjector cavity. Further, in the latter case, the empirical rule in question can be broken more easily because, due to the causality, the cavity radius to be considered is not the physical radius but that of the part of the anode wall around the exit hole reached by the beam electromagnetic influence. We present an analytical treatment of the wakefield driven in a photoinjector by the accelerated electron beam which takes this hole effect into account, whatever the hole radius may be.

## I. INTRODUCTION

Wakefields are usually considered for ultrarelativistic coasting beams. The electromagnetic response of a discontinuous conducting wall to an exciting charged particle is only experienced by the particles located downstream, in the wake. Furthermore, the self-field, or space charge field, is negligible so that the only forces acting on a beam particle are the wakefield and a possible focusing force. At the end, the beam is assumed to be coming from  $-\infty$  and going to  $+\infty$ .

For a photoinjector beam, the situation is very different. It is strongly accelerated from thermal to transrelativistic velocity. If intense, its self-field must be taken into account. In addition, beam electrons appear at the cathode surface at  $t=0$ , the time when laser illumination begins, so that causality governs both synchronous and radiation fields. If it is agreed to call wakefield once again that field experienced by a beam electron which is generated by other beam electrons in the presence of the conducting walls, this wakefield includes both the wall response and the space charge field.

Thus defined wakefield has been analytically calculated for a pill box photoinjector model [1]. Radially, this modelling is relevant because the only parts of the photoinjector RF-cavity walls that the beam field has time to reach, during beam acceleration, are located not far from the axis on both cathode and anode. On the anode however, the question arises of the exit hole influence. The latter has been neglected in [1] by putting forward an empirical rule [2] according to which hole influence is negligible as long as  $r_0/R < 1/3$ , where  $r_0$  and  $R$  are the hole and cavity radii respectively. Though often quoted, this rule is based on a single experimental study worked out



on an ultrarelativistic coasting beam crossing a set of bored cavities. Its validity for the low- to transrelativistic- energy beam accelerated in a photoinjector is questionable.

The aim of the present work is to investigate theoretically the aperture effects on the above defined wakefield.

Fig. 1. Schematic of an RF- photoinjector cavity

## II. EXPANSION OF THE ZONE OF BEAM ELECTROMAGNETIC INFLUENCE: THE THREE PHASES

Before trying to calculate the map  $(\mathbf{E}, \mathbf{B})(\mathbf{x}, t)$  of the beam-generated, time-dependent electromagnetic field, in the presence of the cavity conducting walls, one has to know what parts of these cavity walls are able to play a role in the field map building. Owing to causality, three phases have to be distinguished. In the first:  $t < g/c$  (where  $t=0$  corresponds to the beginning of photoemission) the beam-generated electromagnetic field has not yet reached the exit wall (anode). In the second:  $g/c < t < t_g$ , the beam-generated electromagnetic field has reached the exit wall, but the beam head is still above the exit aperture. In the third:  $t_g < t < t_{gg}$  the beam penetrates the exit hole. For  $E_0=30$  MV/m,  $\tau=30$  ps,  $g=6$  cm, these three phases correspond to:  $t < 200$  ps,  $200 < t < 250$  ps, and  $250 < t < 280$  ps respectively.

## III. FIRST PHASE

The situation is schematized in Fig. 2. The  $(\mathbf{E}, \mathbf{B})(\mathbf{x}, t)$  field map is that already calculated in this phase for the closed cavity [1].

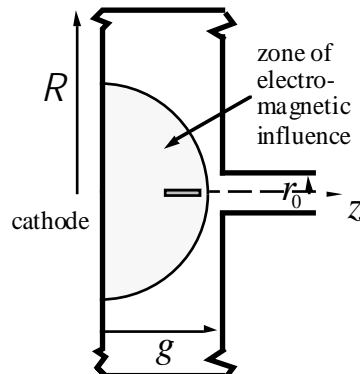


Fig.2. First phase:  $t < g/c$ , where  $t=0$  corresponds to the beginning of photoemission ( $t < 200$  ps for the above parameters)

#### IV. SECOND PHASE

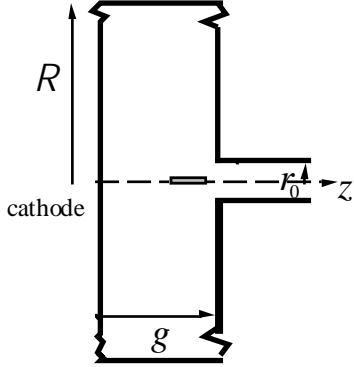


Fig. 3. Second phase:  $g/c < t < t_{qg}$

The question is of solving Maxwell's equations in the unbounded domain of Fig. 3.

There is no rigorous analytical solution which would take into account the boundary conditions of the first step, as well as:

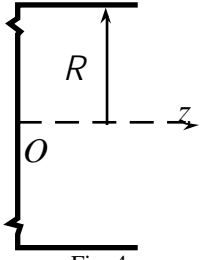
$$\Phi(r_0 \leq r \leq R, z = g, t) = 0,$$

$$A_r(r_0 \leq r \leq R, z = g, t) = 0,$$

and:

$$\frac{\partial A_z}{\partial z}(r_0 \leq r \leq R, z = g, t) = 0.$$

But a good approximation is obtained by assigning these conditions to the general solution in the domain of Fig. 4.



This general solution is the sum of a synchronous field and of a radiation field.

##### A. Synchronous field

This is the particular solution of Maxwell's equations which corresponds to the beam right-hand sides  $\rho(\mathbf{x}, t)$  and  $\mathbf{j}(\mathbf{x}, t)$  (charge and current densities), i.e. in terms of the scalar- and vector-potentials  $\Phi$  and  $\mathbf{A}$ , and in Lorentz gauge:

$$\square \Phi = \rho/\epsilon_0, \quad \square \mathbf{A} = \mu_0 \mathbf{j}.$$

For an axisymmetric radially uniform beam, transformation and Green's function techniques lead to:

$$\Phi_{syn}(r, z, t) = \frac{4I}{\pi^2 \epsilon_0 a R} \sum_{n=1}^{\infty} \frac{J_0(j_n \frac{r}{R}) J_1(j_n \frac{a}{R})}{j_n J_1^2(j_n)} \int_0^{\infty} \frac{\sin(hz)}{h^2 + (\frac{j_n}{R})^2} \times \int_0^t \left[ 1 - \cos\left[c \sqrt{h^2 + (\frac{j_n}{R})^2} (t - t')\right] \right] \left\{ \sin[h(\sqrt{c^2 t'^2 + \Lambda^2} - \Lambda)] - \sin[h(\sqrt{c^2 (t' - \tau)^2 + \Lambda^2} - \Lambda)] \right\} dt' @ h,$$

$$A_{z,syn}(r, z, t) = \frac{4\mu_0 I c}{\pi^2 a R} \sum_{n=1}^{\infty} \frac{J_0(j_n \frac{r}{R}) J_1(j_n \frac{a}{R})}{j_n J_1^2(j_n)} \int_0^{\infty} \frac{\cos(hz)}{h \sqrt{h^2 + (\frac{j_n}{R})^2}} \times \int_0^t \sin\left[c \sqrt{h^2 + (\frac{j_n}{R})^2} (t - t')\right] \left\{ \sin[h(\sqrt{c^2 t'^2 + \Lambda^2} - \Lambda)] - \sin[h(\sqrt{c^2 (t' - \tau)^2 + \Lambda^2} - \Lambda)] \right\} dt' @ h,$$

where  $a$  is the beam radius,  $I$  the current,  $\Lambda = mc^2/eE_0$ , and  $E_0$  the accelerating RF field ( $E_z = -E_0$ ), supposed to be constant during the beam photoemission  $0 \leq t \leq \tau$ , as it is in the 144 MHz cavity of the ELSA photoinjector [3].

##### B. Radiation field

This is a general solution of homogeneous Maxwell's equations. Taking the boundary conditions into account, this general solution can be written under the form:

$$\Phi_{rad}(r, z, t) \propto \sum_{n=1}^{\infty} J_0(j_n \frac{r}{R}) \int_0^{\infty} \sin(hz) \times \left\{ A_{\Phi n}(h) \cos\left(\sqrt{h^2 + \frac{j_n^2}{R^2}} ct\right) + B_{\Phi n}(h) \sin\left(\sqrt{h^2 + \frac{j_n^2}{R^2}} ct\right) \right\} dh,$$

with a similar expression for  $A_{z,rad}$ ,  $\sin(hz)$  being replaced by  $\cos(hz)$ ,  $A_{\Phi n}(h)$  and  $B_{\Phi n}(h)$  by  $A_{An}(h)$  and  $B_{An}(h)$ . These 4 latter functions of  $h$  are, for the time being, arbitrary dimensionless integrable functions, only related by the Lorentz gauge condition which gives:

$$A_{An} = (1/hR) B_{\Phi n}, \quad B_{An} = -(1/hR) A_{\Phi n}.$$

##### C. Calculation of $A_{\Phi n}(h)$ and $B_{\Phi n}(h)$

At first, these integrable functions ( $\int |A_{\Phi n}(h)| dh < \infty$ ) are expanded in Laurent series, taking into account their odd parity ( $A_{\Phi n}(h)$  and  $B_{\Phi n}(h)$  are sin-Fourier coefficients):

$$A_{\Phi n}(h) = (1/hR) \sum_{m=0}^{\infty} A_{\Phi nm} (hR)^{-2m}.$$

To calculate  $A_{\Phi nm}$  and  $B_{\Phi nm}$ , the above boundary condition  $\Phi(r_0 \leq r \leq R, z = g, t)$  is written for  $\Phi_{tot} = \Phi_{syn} + \Phi_{rad}$ , and integrated on  $r$  in its validity domain:  $r_0 \leq r \leq R$ . One is led to an infinite system of linear algebraic equations:

$$\sum_{n=1}^{\infty} \sum_{m=0}^{\infty} \{ \alpha_{nm}(t) A_{\Phi nm} + \beta_{nm}(t) B_{\Phi nm} \} = \zeta(t),$$

where  $\zeta, \alpha_{nm}, \beta_{nm}$  are known functions of  $t$ ,  $A_{\Phi nm}, B_{\Phi nm}$  are the sought after unknowns. A good approximate solution is found by truncating the system to a finite size:  $n \leq N, m \leq M$ , with  $N \sim 100$  and  $M \leq 10$ . The  $2N(M+1)$  unknowns are then calculated by numerically solving the system of  $2N(M+1)$  equations:

$$\sum_{n=1}^N \sum_{m=0}^M \alpha_{nm}(t_i) A_{\Phi nm} + \beta_{nm}(t_i) B_{\Phi nm} = \zeta(t_i), \quad i \in [1, 2N(M+1)],$$

$$t_i \in [g/c, t_g].$$

$A_{\Phi nm}$  and  $B_{\Phi nm}$  being calculated,  $\Phi(r, z, t)$  and  $A_z(r, z, t)$  are

deduced, from which the fields result.

## V. THIRD PHASE

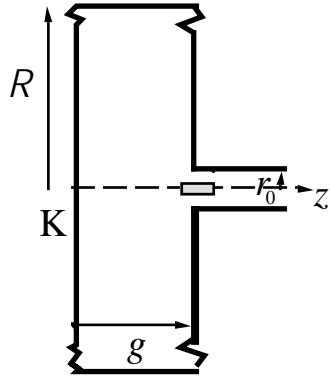


Fig.5. Third phase:  $t_g < t < t_{qg}$

The beam now penetrates the exit hole. The electromagnetic field is obtained by adding, in the cavity and in the drift tube respectively, the synchronous field and a radiation field with undetermined coefficients.

These coefficients are determined, according to the above method, by writing the boundary conditions: a) on the photoinjector anode ( $z = g, r_0 \leq r \leq R$ ) for the

coefficients relative to the field inside the photoinjector, b) on the aperture ( $z = g, 0 \leq r \leq r_0$ ) for the radiation field coefficients inside the drift tube.

### A. Wakefield inside the cavity

#### a) Synchronous field

The techniques used are the same as in phase 2. Again, in Lorentz gauge, one finds for the scalar potential:

$$\begin{aligned} \Phi_{3, photoinj, syn}(r, z, t) &= \frac{4cI}{\pi^2 \epsilon_0 a R} \sum_{n=1}^{\infty} \frac{J_0(j_n \frac{r}{R}) J_1(j_n \frac{a}{R})}{j_n J_1^2(j_n)} \\ &\times \int_0^{\infty} \frac{\sin(hz)}{\sqrt{h^2 + (\frac{j_n}{R})^2}} \times \int_t^{t_g + \tau} \sin[c\sqrt{h^2 + (\frac{j_n}{R})^2} (t \ominus t)] \\ &\times \int_{t \ominus \tau}^{t_g} \sin[h(\sqrt{c^2 t'^2 + \Lambda^2} - \Lambda)] dt' dt \ominus dh, \end{aligned}$$

and for the vector potential:

$$\begin{aligned} A_{z, photoinj, syn}(r, z, t) &= \frac{4\mu_0 c I}{\pi^2 a R} \sum_{n=1}^{\infty} \frac{J_0(j_n \frac{r}{R}) J_1(j_n \frac{a}{R})}{j_n J_1^2(j_n)} \\ &\times \int_0^{\infty} \frac{\cos(hz)}{\sqrt{h^2 + (\frac{j_n}{R})^2}} \int_t^{t_g + \tau} \sin[c\sqrt{h^2 + (\frac{j_n}{R})^2} (t \ominus t)] \\ &\times \left\{ \sin(hg) - \sin[h(\sqrt{c^2 (t \ominus \tau)^2 + \Lambda^2} - \Lambda)] \right\} dt \ominus dh. \end{aligned}$$

### b) Radiation field

This has the same form as in phase 1.

### B. Wakefield inside the drift tube

#### a) Synchronous field

For the scalar potential, the following is found:

$$\begin{aligned} \Phi_{3, tube, syn}(r, z, t) &= \frac{I r_0}{\pi \epsilon_0 c a \beta} \sum_{n=1}^{\infty} \frac{J_0(j_n \frac{r}{r_0}) J_1(j_n \frac{a}{r_0})}{j_n^3 J_1^2(j_n)} \\ &\times \left\{ 2 - \exp[-\frac{j_n}{r_0} (z - g)] - \exp[-\frac{j_n}{r_0} |z - g - \beta c(t - t_g)|] \right\}, \end{aligned}$$

and a similar expression is found for  $A_z$

#### b) Radiation field

The boundary conditions to be satisfied are now:

- $\Phi = 0, A_z = 0$  on the tube wall
- a radiation condition for  $z \rightarrow +\infty$ .

This leads to adopting for the scalar potential:

$$\begin{aligned} \Phi_{3, photoinj, rad}(r, z, t) &\propto \sum_{n=1}^{\infty} J_0(j_n \frac{r}{r_0}) \\ &\times \int_0^{\infty} D_{n\phi}(\omega) \exp[i(\omega t - \sqrt{\frac{\omega^2}{c^2} - \frac{j_n^2}{r_0^2}} z)] d\omega, \end{aligned}$$

with  $\omega > 0$  (wave propagating in the positive z direction).

The unknown functions  $D_{n\phi}(\omega)$ , expanded in Laurent series, are calculated by writing the field continuity on the aperture: ( $z = g, 0 \leq r \leq r_0$ ). After integration on  $r$ , in the interval  $0 \leq r \leq r_0$ , one is led to an infinite system of linear algebraic equations:

$$\sum_{n=1, m=1}^{\infty} K_{n,m}(t) D_{n,m} = L(t)$$

Here again, a good convergence is reached by truncating at  $n_{max} = N$  and  $m_{max} = M$ , with  $N \sim 100$  and  $M \leq 10$ .

Sample field maps are given in a companion paper [4], in which wakefield effects on beam quality are studied.

## REFERENCES

- [1] J.-M. Dolique, EPAC 94, London, UK (1994)
- [2] H. Figuera *et al.*, Phys. Rev. Lett. **60**, 2144 (1988)
- [3] E.g.: S. Joly, J.P. de Brion *et al.*, N.I.M. **A340**, 214 (1994)
- [4] J.-M. Dolique and W. Salah, this conference TPR04